





## LETTER

## Warming advances virus population dynamics in a temperate freshwater plankton community

Thijs Frenken <sup>1,2,3\*</sup> Corina P. D. Brussaard,<sup>4</sup> Mandy Velthuis <sup>1,2,5,6</sup> Ralf Aben,<sup>6</sup> Garabet Kazanjian,<sup>2</sup> Sabine Hilt,<sup>2</sup> Sarian Kosten <sup>1,6</sup> Edwin T. H. M. Peeters,<sup>7</sup> Lisette N. de Senerpont Domis,<sup>1,7</sup> Susanne Stephan,<sup>8</sup> Ellen van Donk,<sup>1,9</sup> Dedmer B. Van de Waal <sup>1</sup>

<sup>1</sup>Department of Aquatic Ecology, Netherlands Institute of Ecology (NIOO-KNAW), Wageningen, The Netherlands;

<sup>2</sup>Department of Ecosystem Research, Leibniz-Institute of Freshwater Ecology and Inland Fisheries (IGB), Berlin, Germany;

<sup>3</sup>Great Lakes Institute for Environmental Research (GLIER), University of Windsor, Windsor, Ontario, Canada;

<sup>4</sup>Department of Marine Microbiology and Biogeochemistry, Royal Netherland Institute for Sea Research (NIOZ), University of Utrecht, Den Burg, The Netherlands; <sup>5</sup>Division Water and Food, Wageningen Environmental Research, Wageningen University and Research (WUR), Wageningen, The Netherlands; <sup>6</sup>Department of Aquatic Ecology and Environmental Biology, Institute for Water and Wetland Research, Radboud University Nijmegen (RU), Nijmegen, The Netherlands;

<sup>7</sup>Department of Aquatic Ecology and Water Quality Management, Wageningen University and Research (WUR), Wageningen, The Netherlands; <sup>8</sup>Department of Experimental Limnology, Leibniz-Institute of Freshwater Ecology and Inland Fisheries (IGB), Stechlin, Germany; <sup>9</sup>Department of Biology, University of Utrecht (UU), Utrecht, The Netherlands

### Scientific Significance Statement

Viruses are the most abundant biological entities on earth and play an important role in carbon and nutrient cycling in aquatic ecosystems. Laboratory studies have shown that warming can stimulate phytoplankton growth, and thereby trigger an increased production of their viruses. It remains unclear how warming will affect host-virus dynamics in more complex natural plankton communities over longer time periods, particularly in freshwater systems. Our results demonstrated for the first time that warming advances the timing of virus population dynamics, but neither changed peak nor time-integrated number of viruses. Although warming may not result in a stronger viral control of natural bacterial and phytoplankton communities, it can alter timing of host-virus interactions, and thus the timing of carbon and nutrient recycling.

Viruses are important drivers in the cycling of carbon and nutrients in aquatic ecosystems. Since viruses are obligate parasites, their production completely depends on growth and metabolism of hosts and therefore can be affected by climate change. Here, we investigated if warming (+4°C) can change the outcome of viral infections in a natural freshwater virus community over a 5-month period in a mesocosm experiment. We monitored dynamics of viruses and potential hosts. Results show that warming significantly advanced the early

\*Correspondence: T.Frenken@nioo.knaw.nl

Associate editor: James Cloern

**Author Contribution Statement:** T.F., M.V., R.A., and G.K. performed the experiment. T.F. and C.B. performed virus and bacteria counts. M.V. performed phytoplankton counts. R.A. and S.K. performed DOC analyses. G.K. and S.H. performed periphyton analyses. T.F., M.V., C.B., and D.V.W. analyzed the data. M.V. and T.F. performed statistical analyses. T.F., D.V.W., and C.B. wrote the first draft of the manuscript. All authors were involved in the design of the experiment and contributed to improving the manuscript.

**Data Availability Statement:** Data available via <https://hdl.handle.net/10411/LLRREO>; code available via <https://datadryad.org/stash/dataset/doi:10.5061/dryad.6tv0f>

Additional Supporting Information may be found in the online version of this article.

This is an open access article under the terms of the Creative Commons Attribution License, which permits use, distribution and reproduction in any medium, provided the original work is properly cited.

summer peak of the virus community by 24 d, but neither affected viral peak abundances nor time-integrated number of viruses present. Our results demonstrate that warming advances the timing of viruses in a natural community. Although warming may not necessarily result in a stronger viral control of bacterial and phytoplankton communities, our results suggest it can alter host population dynamics through advanced timing of infections, and thus timing of carbon and nutrient recycling.

Viruses are important players in the cycling of carbon and nutrients in aquatic ecosystems (Suttle 2007). After viruses lyse microbial hosts, organic carbon and nutrients are released into the water, supporting new bacterial and phytoplankton growth via the viral shunt (Bratbak et al. 1998; Wilhelm and Suttle 1999; Brussaard et al. 2005; Lønborg et al. 2013). Hereby viruses can control host population densities, as well as steer overall aquatic microbial community diversity (Fuhrman 1999; Brussaard 2004b; Suttle 2007). In natural bacterioplankton communities, viral abundance has been shown to covary with environmental factors such as phosphorus (P), dissolved organic carbon (DOC), and temperature (Lymer et al. 2008). These conditions primarily affect host physiology, and thereby may influence virus replication or infection success. For example, earlier work has shown that under resource limitation host growth can be constrained, thereby prolonging virus latent period and/or resulting in a reduced burst size (Maat et al. 2016; Maat and Brussaard 2016; Cheng et al. 2019). Warming has been reported to stimulate host growth rates and, as such, virus production (Steenhauer et al. 2016; Demory et al. 2017; Maat et al. 2017). These studies mainly focused on single-species host cultures and virus isolates, while little is known about the effects of warming on virus dynamics in more complex freshwater food webs containing a suite of phytoplankton and bacterial hosts.

Here, we investigated the impacts of warming on virus community dynamics in a natural temperate freshwater plankton community over a spring to summer period (March–August) under controlled experimental conditions. We performed an experiment using fishless indoor mesocosms (~ 1000 liter) with natural lake sediment. Mesocosms were programmed to follow a seasonal temperate (control;  $n = 4$ ) and a warmed (+ 4°C;  $n = 4$ ) temperature scenario (IPCC scenario RCP6.0; Stocker 2014). The systems were inoculated with plankton and sediment from a nearby pond and were sampled weekly or twice every week providing a high temporal resolution (for details, see Velthuis et al. 2017). Based on data from the same mesocosm experiment, we have shown earlier that warming led to reduced phytoplankton biomass as well as a temporarily higher periphyton production in spring (Velthuis et al. 2017; Kazanjian et al. 2018). Moreover, we have shown that warming led to an advanced timing of fungal parasite infections during the spring diatom bloom (Frenken et al. 2016). Senescence of these various primary producers will provide organic substrate available to heterotrophic bacteria, which are numerically the dominant host organisms for viruses (Weinbauer 2004; Wigington et al. 2016). Since warming may lead to increased metabolic rates of heterotrophic

bacteria (Brown et al. 2004; Price and Sowers 2004), we hypothesize that temperature-driven increases in bacterial metabolic rates will enhance virus production, leading to increased aquatic virus production and a stronger viral control of microbial host dynamics.

## Results

The total virus community dynamics showed a clear seasonal pattern, with a distinct increase starting in early May (Fig. 1A). Warming did not significantly affect virus peak height or the time-integrated number of viruses present over the duration of the experiment (Supporting Information Table S1). However, we did observe a significant time-dependent effect of warming on total virus abundance (time  $\times$  treatment effect,  $p < 0.001$ ; Supporting Information Table S2), where the timing of the virus peak advanced with about 24 d ( $p < 0.05$ ; Table 1). Five separate virus groups could be distinguished using flow cytometry (Supporting Information Fig. S1). Viral groups with a lower nucleic acid-specific fluorescence signal (V1–V3) are generally considered to infect bacteria (Brussaard 2004a; Mojica et al. 2015). During our experiment, V1–V3 showed similar dynamics, with a stronger increase at the start of May in the warmer mesocosms as compared to the controls (Fig. 1B–D). Groups V4 and V5 are typically associated to double stranded DNA eukaryotic algal viruses (Brussaard et al. 2000; Brussaard 2004a). Their abundances showed two peaks, the first in April/May and a second in July (Fig. 1E,F). The standing stock of heterotrophic bacteria in the warm mesocosms tended to be higher than in controls (treatment effect,  $p = 0.055$ , Supporting Information Table S2), mainly during the spring bloom (Fig. 2A). Warming did not significantly affect DOC concentration, although it showed a distinct seasonal pattern (Fig. 2B, Supporting Information Table S2). Warming resulted in a lower density of phytoplankton cells (Velthuis et al. 2017), as well as a reduced seston chlorophyll *a* (Chl *a*) concentration that reached maximum values of  $32.6 \pm 3.5$  and  $27.5 \pm 4.8 \mu\text{g L}^{-1}$  (mean  $\pm$  SE) in the control and warm treatment, respectively (Fig. 2C; Supporting Information Tables S2, S3). The phytoplankton spring bloom consisted mainly of relatively large-sized algae, in the size range 30–85  $\mu\text{m}$ , and was dominated by the diatom *Synedra* sp., while afterwards it was dominated by pico- and nano-sized phytoplankton, in the size fractions  $< 2$  and 2–30  $\mu\text{m}$ , respectively (Frenken et al. 2016; Velthuis et al. 2017). The output of the linear model (Table 2) indicates

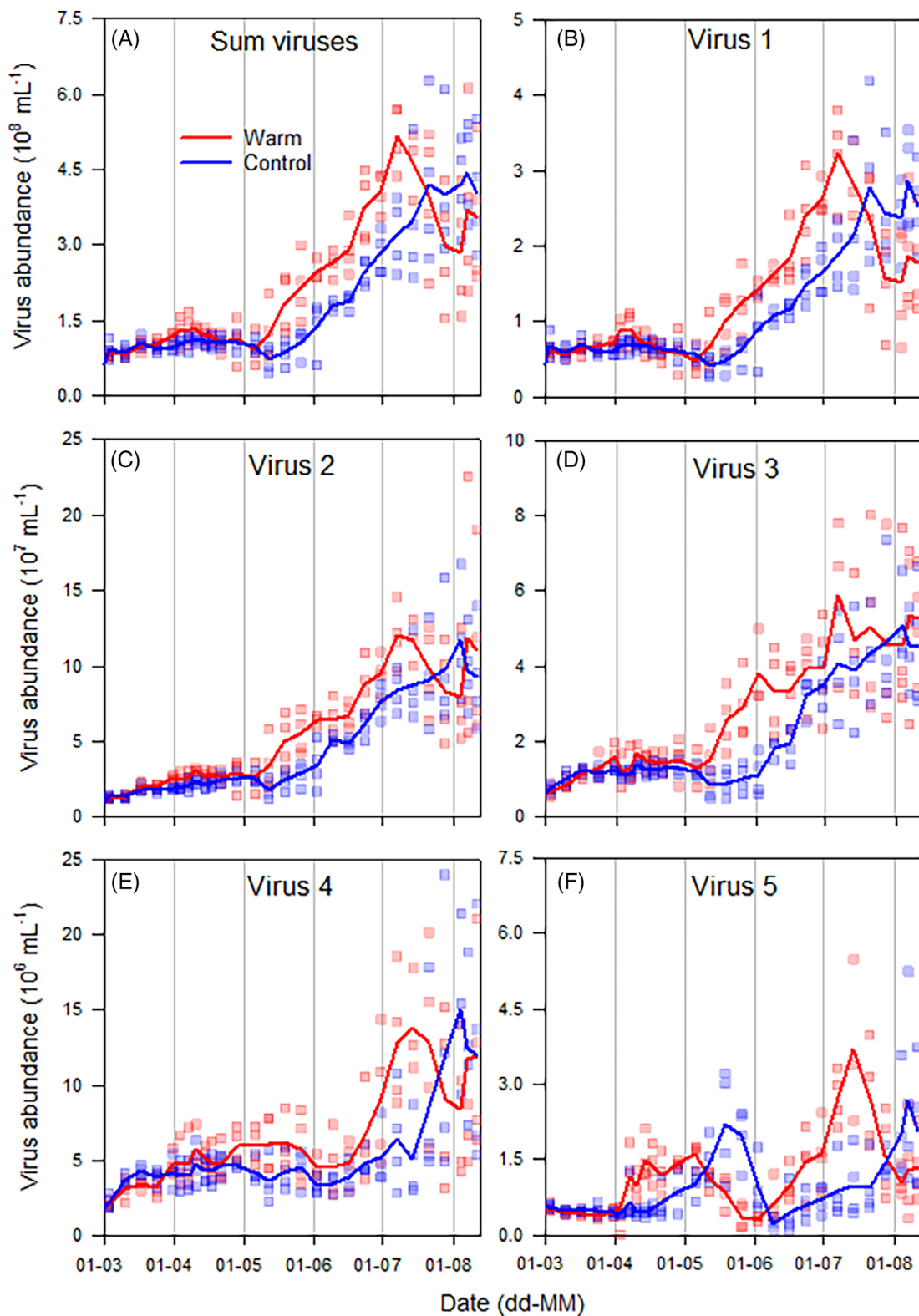


**Fig 1.** Dynamics of the total virus abundances (A) and abundances of different virus groups (B–F) over the course of the experiment. Symbols denote replicates, with the solid lines indicating the average for each treatment across replicates ( $n = 4$ ). Axes are on different scales for clarity. Virus groups were separated based on their fluorescence.

**Table 1** Summary output of Weibull fits reporting shifts in peak timing of viruses (*peak*) and when half of this peak was reached (*half max*), in response to warming.

Variable	Peak nr.	Shifts in peak timing(days)	
		Peak	Half max
Sum viruses	1	<b>-23.8</b>	<b>-24.0</b>
Virus 1	1	<b>-23.3</b>	<b>-19.8</b>
Virus 2	1	-17.0	<b>-31.3</b>
Virus 3	1	-17.8	<b>-30.3</b>
Virus 4	1	<b>-26.0</b>	<b>-28.5</b>
Virus 5	1	-19.0	<b>-24.3</b>
	2	<b>-26.0</b>	<b>-22.5</b>

Bold values indicate significant response to warming ( $p < 0.05$ ).

that the abundance of heterotrophic bacteria and prokaryotic nanophytoplankton (i.e., nano-sized cyanobacteria) generally contributed most to explaining the observed dynamics in the different virus groups. Furthermore, we did not observe an effect of treatment on the contribution of the different variables (i.e., potential virus hosts) in explaining the total variance in the dynamics of the total virus community dynamics nor any of the individual virus groups (Table 2).

## Discussion

Warming resulted in an advanced peak timing of the virus community in a complex plankton food web. The relative contribution of prokaryotic pico- and nanophytoplankton (i.e., pico- and nano-sized cyanobacteria) to the viral dynamics was higher than that of the heterotrophic bacteria (Table 2). Yet, heterotrophic bacterial abundances were at least two orders of magnitude higher (Fig. 2A), and therefore likely served as the main viral hosts, contributing most to the actual number of viruses produced. This is exemplified by the total virus-to-bacteria ratio (VBR, Supporting Information Fig. S2), ranging on average between 20 and 85, which is in the typical range for freshwater systems (Maranger and Bird 1995; Wommack and Colwell 2000).

The standing stock of heterotrophic bacteria in the warmer mesocosms tended to be higher than in controls, which may possibly result from higher bacterial growth rates. Although we did not assess bacterial growth rates directly in our experiment, net community growth rates indeed seemed to be higher in the warm treatment during two different periods of the experiment as compared to the control (Supporting Information Table S4). Temperature can enhance bacterial production and growth rates (Schultz et al. 2003; Price and Sowers 2004; Lymer et al. 2008), but also shorten virus latent period and increase burst size, thereby increasing virus production (Steenhauer et al. 2016; Cheng et al. 2017; Maat et al. 2017). This could possibly explain the overall advanced

timing of viruses during early May in the warmer mesocosms as compared to the controls (Fig. 2A). The concomitantly earlier and steeper increase in VBR that we observed in the warm treatments (Supporting Information Fig. S2) indicates a strong viral control on the bacterial community during May.

Viruses were not able to prevent a second distinct increase in bacterial abundances (constant and comparable average VBR in June for both warmer mesocosms and controls; Supporting Information Fig. S2); however, the higher bacterial net growth rates in the warmer mesocosms resulted in enhanced bacterial standing stock (Fig. 2A). The bacterial community may have changed over time, allowing a temporary escape from viral control. Alternatively, viral infectivity may have dropped due to prolonged warming. While the temperature tolerance of viruses is usually wider than that of their respective hosts (Mojica and Brussaard 2014), temperature has been reported to reduce viral infectivity and thus negating the virus' ability to successfully infect their hosts (Nagasaki and Yamaguchi 1998; Baudoux and Brussaard 2008; Maat et al. 2017). Besides direct warming effects, temperature-dependent changes in other factors, such as ultraviolet light and attachment to inorganic and organic particles, may have affected viral decay rates (Mojica and Brussaard 2014; Long and Short 2016; Maat et al. 2019). For example, the drop in virus abundance in the warm mesocosms in July may have resulted from the advanced bacterial infections (and a lower VBR), possibly releasing higher amounts of suspended particles into the water. In our experiments however, DOC concentrations did not change in response to warming, and light conditions were the same in all mesocosms.

We identified five groups of viruses based on their size and fluorescence characteristics. Although the nucleic acid-specific dye used is sensitive, we still may have somewhat underestimated the number of the smallest genome V1 viruses as a result of the flow cytometric detection limits (Brussaard et al. 2000; Tomaru and Nagasaki 2007). Furthermore, the observed temporal dynamics of V1 and the other virus groups were comparable, suggesting a consistent response of the different viruses towards temperature-driven shifts in host dynamics. To elucidate the influence of warming on virus diversity within the distinct virus clusters, we recommend future research to include molecular identification of the sorted virus groups.

Abundances of bacteria showed an initial decline at the start of the experiment, presumably because insufficient organic substrate was available at the start of the experiment (Fig. 2A,B). Afterward, bacterial numbers largely followed the temporal dynamics in DOC concentration (Fig. 2A,B). The DOC concentrations showed a distinct seasonal pattern with an initial peak in April that seems related to the decline of the phytoplankton spring bloom (Fig. 2B,C). The termination of the phytoplankton spring bloom was accelerated in the warm treatment, possibly induced by fungal parasites (Frenken et al. 2016) combined with nutrient limitation, grazing, and

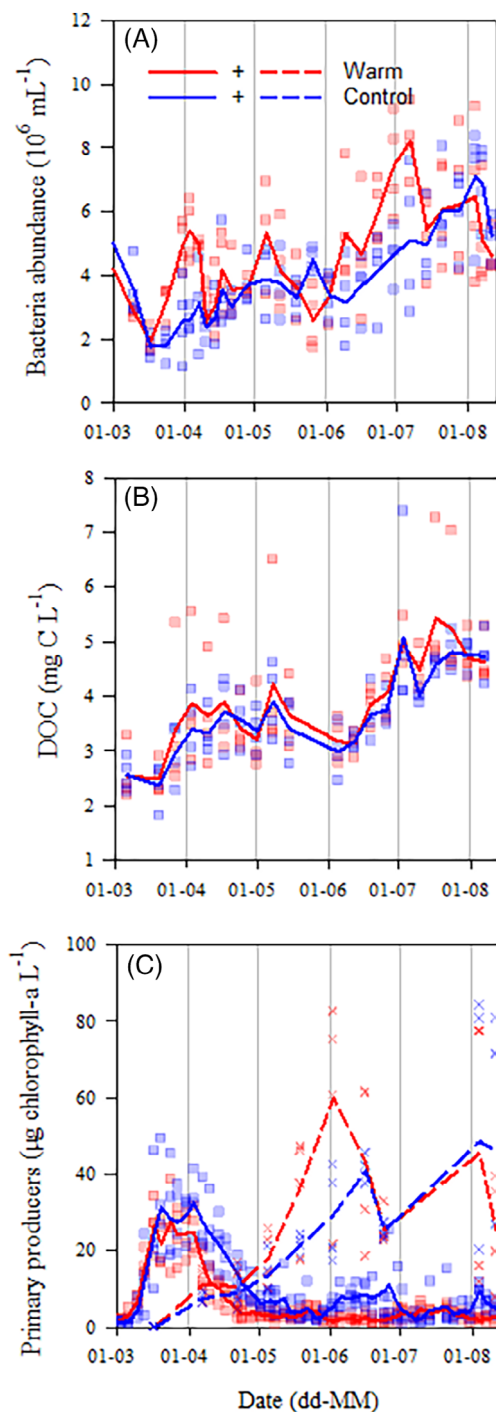


**Fig 2.** Dynamics of heterotrophic bacteria abundances (A), DOC concentration (B), phytoplankton (squared symbol and solid lines) abundances, and periphyton (cross symbol and dashed lines) biomass (C) over the course of the experiment. Symbols denote replicates, with the solid lines indicating the average for each treatment across replicates ( $n = 4$ ).

viral infection (Figs. 1 and 2). Afterward, phytoplankton biomass remained relatively low, likely due to advanced zooplankton grazing pressure and enhanced competition for

nutrients with periphyton (Velthuis et al. 2017; Kazanjian et al. 2018). A second increase in DOC in June–July seems related to the decline in periphytic algae (Fig. 2B,C), which were the dominant primary producers after May with maximum biomass, as normalized Chl *a* concentrations, of  $48.6 \pm 19.6$  and  $59.9 \pm 13.6 \mu\text{g L}^{-1}$  (mean  $\pm$  SE; see also Kazanjian et al. 2018) in the control and warm treatments, respectively (Fig. 2C).

Our experimental results suggest a coupling between the dynamics in viruses, bacteria, and primary producers-derived DOC and show largely consistent effects of warming among different virus groups. Pico- and nano-phytoplankton, notably cyanobacteria, possibly served as hosts to viruses directly, while micro-phytoplankton and periphyton could have provided DOC for heterotrophic bacteria that, in turn, acted as predominant viral hosts. Moreover, warming resulted in advanced timing of all observed virus groups, but neither changed peak height nor the time-integrated number of viruses present. This implies that although warming clearly affects the interaction between hosts and parasites in single isolates (as shown by Demory et al. 2017; Maat et al. 2017), it does not necessarily lead to a stronger viral control of natural bacterioplankton communities in complex food webs. Our results suggest that both direct and indirect mechanisms may contribute to explaining the observed temperature-driven shifts in timing of virus populations under global warming. Although warming may not necessarily result in a stronger viral control of natural bacteria and phytoplankton communities, it can alter timing of host-virus interactions, and thus alter the timing of carbon and nutrient recycling.

## Materials and methods

### Experimental setup

Experiments were carried out in indoor mesocosms (from now on referred to as “limnotrons”), where temperature, light, and mixing conditions can be set within narrow limits. With an average depth of 1.35 m and an inner diameter of 0.97 m (Verschoor et al. 2003) the total working volume is about 988 L. In this study, we present data from the start of the experiment on 3 March 2014 until 11 August 2014. For details on the experimental setup, see Velthuis et al. (2017). In short, each limnotron was filled with 80 liters of homogenized and sieved sediment from two small ponds in Wageningen, the Netherlands, 2 weeks prior to start of the experiment. Then, each limnotron was filled with tap water and spiked with a concentrated plankton assemblage ( $\geq 30 \mu\text{m}$ ) retrieved by concentrating 300 liters of water from the same ponds as where the sediment was taken from. To accommodate gas exchange and mixing, two compact axial fans (AC axial compact fan 4850 Z, ebm-papst St. Georgen GmbH, KG, Georgen, Germany) and an aquarium pump (EHEIM compact 300, EHEIM GmbH, KG, Deizisau, Germany) were installed and set at a rate of  $100 \text{ m}^3 \text{ h}^{-1}$  and  $150 \text{ L h}^{-1}$ , respectively. Together, these fans and pump

**Table 2** Average relative contribution (as a fraction of one) of potential host (bacterial and phytoplankton groups) to the explanation of the variability of different virus time series dynamics (expressed as contribution to the total  $R^2$  of linear models) in the control and warm treatments ( $n = 4$ ).

Treatments	Phytoplankton												
	Heterotrophic bacteria				Prokaryotes				Eukaryotes				
	Average	SD	Average	SD	< 2 $\mu\text{m}$	2–30 $\mu\text{m}$	30–85 $\mu\text{m}$	< 2 $\mu\text{m}$	2–30 $\mu\text{m}$	30–85 $\mu\text{m}$	Average	SD	
Control	Sum viruses	0.18	0.05	0.19	0.03	0.29	0.04	0.06	0.01	0.03	0.03	0.02	0.01
	Virus 1	0.15	0.09	0.20	0.03	0.26	0.07	0.05	0.01	0.02	0.02	0.03	0.01
	Virus 2	0.20	0.04	0.22	0.08	0.25	0.05	0.05	0.02	0.04	0.05	0.04	0.03
	Virus 3	0.18	0.07	0.19	0.04	0.27	0.03	0.07	0.01	0.04	0.03	0.02	0.01
	Virus 4	0.14	0.06	0.17	0.08	0.25	0.04	0.03	0.02	0.02	0.01	0.04	0.03
Warm	Sum viruses	0.20	0.06	0.10	0.05	0.15	0.12	0.01	0.02	0.04	0.03	0.03	0.01
	Virus 1	0.25	0.08	0.06	0.04	0.07	0.06	0.05	0.03	0.11	0.06	0.06	0.04
	Virus 2	0.15	0.04	0.11	0.05	0.20	0.13	0.04	0.02	0.14	0.05	0.07	0.03
	Virus 3	0.13	0.06	0.12	0.03	0.22	0.05	0.05	0.03	0.08	0.06	0.06	0.05
	Virus 4	0.15	0.07	0.16	0.08	0.21	0.19	0.03	0.01	0.07	0.07	0.05	0.02
Virus 5	0.11	0.04	0.16	0.11	0.09	0.05	0.04	0.05	0.12	0.01	0.04	0.01	

The contribution of the specific host groups to the explanation of the virus dynamics was similar in the control and the warmed treatment. SD, standard deviation.

provided mixing and prevented stratification. The temperature and light scenario resembled natural seasonality (control,  $n = 4$ ) based on average Dutch conditions and a warmed treatment ( $+4^{\circ}\text{C}$ , IPCC scenario RCP6.0; Stocker 2014).

We note that a small part of the data reported in our study (Fig. 2C, part of data in Supporting Information Table S2) have been published earlier (Frenken et al. 2016; Velthuis et al. 2017; Kazanjian et al. 2018). Here, we focus on virus dynamics and show novel data on the dynamics in various virus groups, phytoplankton community, bacteria, and DOC (Figs. 1, 2A,B, Supporting Information Figs. S1, S2; Supporting Information Tables S1–S3). We reported earlier findings because these are potential controlling factors for viruses, including phytoplankton and periphyton biomass (Chl *a*), as these may provide potential hosts, and also because these were the dominant primary producers and thus produce DOC that provides substrate to heterotrophic bacteria, which are predominant hosts.

### Sample analyses

All water and plankton analyses were performed on depth-integrated samples taken from the limnotrons using a custom-made Plexiglas cylindrical tube sampler with a volume of 3.5 liters. Depth-integrated samples were taken from the upper meter and were homogenized before subsampling.

### Bacteria, virus, and phytoplankton enumeration by flow cytometry

Flowcytometric detection of algae, bacteria, and viruses are established methods that are based on detecting and measuring their individual optical and fluorescent properties (natural pigments such as Chl *a* or phycocyanin in the case of prokaryotic and eukaryotic phytoplankton; and after staining with fluorescent dyes in the case of bacteria and viruses), and is widely used in plankton ecological studies (Brussaard et al. 2005; Jacquet et al. 2002; Peter and Sommer 2013; Tjeldens et al. 2008; Velthuis et al. 2017).

Bacteria and viruses were enumerated after staining with a green fluorescent nucleic acid-specific dye (SYBR Green I) in combination with flow cytometry. For bacteria, the staining assay by Marie et al. (1999) was used and for viruses the method by Brussaard (2004a), which was optimized for better staining (Mojica et al. 2014). In short, 2 mL was subsampled from the depth integrated sample once or twice a week and was fixed with glutaraldehyde (25% EM grade) to a final concentration of 0.5% for 30 min, where after the sample was flash-frozen in liquid nitrogen and stored at  $-80^{\circ}\text{C}$ . Samples were thawed just before analysis, and diluted in a Tris-EDTA buffer (pH 8.2) and stained with SYBR Green I (final concentration of  $5 \times 10^{-5}$  of commercial stock) for 15 min in the dark at room temperature for bacteria and 10 min at  $80^{\circ}\text{C}$  for viruses. Subsequently, the virus samples were left to cool at room temperature for 5 min before analysis. We used a FACSCalibur flow cytometer (BD FACSCalibur, BD Biosciences, San Jose, CA) equipped with a 488-nm argon laser at a voltage of 15-mW and

the standard filter setup. Samples were analyzed with discriminator set on the green fluorescence ( $520 \pm 20$  nm). Flow cytometric data were analyzed using the program Flowing Software 2.5.1. (freely available from [www.flowingsoftware.com](http://www.flowingsoftware.com)). Bacteria and viruses (five distinct virus groups V1–V5) were identified based on their green fluorescent staining and side scatter characteristics (Supporting Information Fig. S1). Using this approach, the (numerically dominant) viruses are distinct from low nucleic acid content bacteria (i.e., LNA bacteria or ultramicrobacteria; Liu et al. 2017, Proctor et al. 2018) and potential giant viruses (Khalil et al. 2017; Deeg et al. 2018).

To assess phytoplankton abundance, 4 mL was subsampled from the depth integrated sample twice a week and fixed with a paraformaldehyde–glutaraldehyde solution to final concentrations of 0.025% and 0.0037% by mass, respectively, and stored at  $5^{\circ}\text{C}$  for a maximum period of 6 weeks prior to analysis. Samples were prefiltered through an  $85\text{-}\mu\text{m}$  mesh filter and analyzed on a MoFlo XDP flow cytometer (Beckman Coulter Nederland BV, Woerden, the Netherlands) equipped with a 488- and 647-nm laser operated at 120 and 55 mW, respectively (Dijk et al. 2010). Red autofluorescence (using the 488 nm laser) was used to discriminate Chl *a* ( $670 \pm 30$  nm) containing photoautotrophs and additionally, the 647-nm laser allowed to differentiate for phycocyanin containing cyanobacteria ( $675 \pm 30$  nm). We note that not all cyanobacteria contain phycocyanin, but phycocyanin containing cyanobacteria are often the dominant cyanobacterial group in these freshwaters (Pick 1991; Callieri et al. 2012). Thus, we counted all photoautotrophs with Chl *a* (thus including all cyanobacteria) and additionally report specifically the phycocyanin-containing cyanobacteria. Water samples were size-fractionated into three size classes ( $< 2$ ,  $2\text{--}30$  and  $30\text{--}85\ \mu\text{m}$ ) based on the forward scatter of  $2\text{-}$  and  $30\text{-}\mu\text{m}$  beads.

### Chl *a* analysis

For Chl *a* measurements, samples were filtered over a  $220\text{-}\mu\text{m}$  mesh and analyzed in triplicate on a Phyto-PAM with an Optical Unit ED-101US/MP (Heinz Walz GmbH, Effeltrich, Germany). These data were calibrated with spectrophotometric measurements of Chl *a* after ethanol extractions performed at various days during the entire experimental period ( $R^2 = 0.68$ ;  $n = 189$ ;  $p < 0.001$ ). For more details, see Frenken et al. (2016).

To determine periphyton biomass, transparent polypropylene strips ( $10 \times 1.3$  cm) with textured surfaces (IBICO, GBC, Chicago, IL) were placed in the limnotrons at two different depths (10 and 60 cm below water surface). Chl *a* was used as a proxy for primary producer biomass, which was analyzed in triplicate biweekly using high-performance liquid chromatography (Waters, Millford, MA) following the methods described in Köhler et al. (2010). Total periphytic biomass was calculated by multiplying the average Chl *a* concentrations from the two depths with the total limnotron wall surface area ( $4.02\ \text{m}^2$ ). To allow a direct comparison between different

primary producers, a proxy for the periphyton concentration in each limnotron was calculated by dividing the total wall Chl *a* by the total volume of water.

### DOC measurements

For DOC measurements, a subsample of the integrated water sample was filtered through a rhizon (0.15  $\mu\text{m}$ , rhizosphere Research Products B.V., Wageningen, the Netherlands) and analyzed on a TOC-L CPH/CPN analyzer (Shimadzu, Kyoto, Japan).

### Statistical analyses

Viral, bacterial, and phytoplankton abundances, as well as DOC and periphyton biomass were tested for effect of treatment, time, and their interaction by repeated-measures analysis of variance (ANOVA) using the statistical package IBM SPSS Statistics 25 (IBM Corporation, New York, NY). We note that the statistical output for the effect of warming on different phytoplankton groups and size classes (Supporting Information Table S3) is different from that presented in Velthuis et al. (2017). These differences are the result of the different statistical analyses performed. Supporting Information Table S3 shows specifically the different size classes within the categories of prokaryotic and eukaryotic phytoplankton, while Velthuis et al. (2017) report the total size classes (i.e., the sum of prokaryotic and eukaryotic phytoplankton). For viral dynamics, the cardinal dates where viral abundances were over 50% from the maximum measured abundance and peak timing in that specific limnotron were estimated by fitting the data points with a Weibull function (Rolinski et al. 2007) in R (version 3.2.5) for statistical computing (R Core Team 2013) using the package “carddates.” In this way, it is possible to test for potential timing related changes in virus population dynamics. Cardinal dates were statistically compared between treatments using a *t* test in the statistical package SigmaPlot for Windows version 12.5 (Systat Software, London, UK).

General linear models were used to explore the relationship of each virus group with potential host organisms (heterotrophic bacteria, prokaryote and eukaryote phytoplankton of 0–2, 2–30, and 30–85  $\mu\text{m}$  size classes). Missing values were interpolated with the *na.spline* function from the package “zoo.” We checked for the presence of nonstationarity in all mesocosm time series by testing the residuals from the model fits with the function *auto.arima* (package *forecast* from Hyndman 2015). If nonstationarity was present, we removed this temporal autocorrelation by ARIMA transformation (Supporting Information Table S5). Subsequently, we proceeded with the stationary time series to assess the relative contribution of each of the potential host organisms to the total  $R^2$  of the mesocosm specific models for each virus group separately. This analysis was carried out using the function *calc.relimp.lm* from the package “relaimpo.” Relative contribution per variable was then tested within model fits and between treatments using two-way ANOVA.

### References

- Baudoux, A.-C., and C. P. D. Brussaard. 2008. Influence of irradiation on virus–algal interactions. *J. Phycol.* **44**: 902–908.
- Bratbak, G., A. Jacobsen, and M. Heldal. 1998. Viral lysis of *Phaeocystis pouchetii* and bacterial secondary production. *Aquat. Microb. Ecol.* **16**: 11–16.
- Brown, J. H., J. F. Gillooly, A. P. Allen, V. M. Savage, and G. B. West. 2004. Toward a metabolic theory of ecology. *Ecology* **85**: 1771–1789.
- Brussaard, C. P. D. 2004a. Optimization of procedures for counting viruses by flow cytometry. *Appl. Environ. Microbiol.* **70**: 1506–1513.
- Brussaard, C. P. D. 2004b. Viral control of phytoplankton populations—A review. *J. Eukaryot. Microbiol.* **51**: 125–138.
- Brussaard, C. P. D., D. Marie, and G. Bratbak. 2000. Flow cytometric detection of viruses. *J. Virol. Methods* **85**: 175–182.
- Brussaard, C. P. D., B. Kuipers, and M. J. W. Veldhuis. 2005. A mesocosm study of *Phaeocystis globosa* population dynamics: I. Regulatory role of viruses in bloom control. *Harmful Algae* **4**: 859–874.
- Callieri, C., G. Cronberg, and J. G. Stockner. 2012. Freshwater picocyanobacteria: Single cells, microcolonies and colonial forms, p. 229–269. In *Ecology of cyanobacteria II*. Dordrecht: Springer.
- Cheng, K., D. B. Van de Waal, X. Y. Niu, and Y. J. Zhao. 2017. Combined effects of elevated pCO<sub>2</sub> and warming facilitate cyanophage infections. *Front. Microbiol.* **8**: 1096.
- Cheng, K., T. Frenken, C. P. D. Brussaard, and D. B. Van de Waal. 2019. Cyanophage propagation in the freshwater cyanobacterium *Phormidium* is constrained by phosphorus limitation and enhanced by elevated pCO<sub>2</sub>. *Front. Microbiol.* **10**: 617.
- Deeg, C. M., C. E. T. Chow, and C. A. Suttle. 2018. The kinetoplastid-infecting bodo saltans virus (Bsv), a window into the most abundant giant viruses in the sea. *Elife* **7**: 1–22. doi:10.7554/eLife.33014.
- Demory, D., and others. 2017. Temperature is a key factor in *Micromonas*–virus interactions. *ISME J.* **11**: 601.
- Frenken, T., and others. 2016. Warming accelerates termination of a phytoplankton spring bloom by fungal parasites. *Glob. Chang. Biol.* **22**: 299–309.
- Fuhrman, J. A. 1999. Marine viruses and their biogeochemical and ecological effects. *Nature* **399**: 541–548.
- Hyndman, R. J. 2015. *{Forecast}: Forecasting functions for time series and linear models. R package version 6.2.* <https://github.com/robjhyndman/forecast>
- Jacquet, S., M. Heldal, D. Iglesias-Rodriguez, A. Larsen, W. Wilson, and G. Bratbak. 2002. Flow cytometric analysis of an *Emiliana huxleyi* bloom terminated by viral infection. *Aquat. Microb. Ecol.* **27**: 111–124.
- Kazanjian, G., and others. 2018. Impacts of warming on top-down and bottom-up controls of periphyton production. *Sci. Rep.* **8**: 9901.



- Khalil, J. Y. B., and others. 2017. Flow cytometry sorting to separate viable giant viruses from amoeba co-culture supernatants. *Front. Cell. Infect. Microbiol.* **6**: 1–10.
- Köhler, J., J. Hachoł, and S. Hilt. 2010. Regulation of submersed macrophyte biomass in a temperate lowland river: Interactions between shading by bank vegetation, epiphyton and water turbidity. *Aquat. Bot.* **92**: 129–136.
- Liu, J., and others. 2017. Geographic distribution pattern of low and high nucleic acid content bacteria on a river-catchment scale. *Mar. Freshw. Res.* **68**: 1618–1625.
- Lønborg, C., M. Middelboe, and C. P. D. Brussaard. 2013. Viral lysis of *Micromonas pusilla*: Impacts on dissolved organic matter production and composition. *Biogeochemistry* **116**: 231–240.
- Long, A. M., and S. M. Short. 2016. Seasonal determinations of algal virus decay rates reveal overwintering in a temperate freshwater pond. *ISME J.* **10**: 1602–1612.
- Lymer, D., J. B. Logue, C. P. D. Brussaard, A.-C. Baudoux, K. Vrede, and E. S. Lindström. 2008. Temporal variation in freshwater viral and bacterial community composition. *Freshw. Biol.* **53**: 1163–1175.
- Maat, D., and others. 2017. Characterization and temperature dependence of Arctic *Micromonas polaris* viruses. *Viruses* **9**: 134.
- Maat, D. S., and C. P. D. Brussaard. 2016. Both phosphorus and nitrogen limitation constrain viral proliferation in marine phytoplankton. *Aquat. Microb. Ecol.* **77**: 87–97.
- Maat, D. S., R. de Blok, and C. P. D. Brussaard. 2016. Combined phosphorus limitation and light stress prevent viral proliferation in the phytoplankton species *Phaeocystis globosa*, but not in *Micromonas pusilla*. *Front. Mar. Sci.* **3**: 160.
- Maat, D. S., M. A. Prins, and C. P. D. Brussaard. 2019. Sediments from arctic tide-water glaciers remove coastal marine viruses and delay host infection. *Viruses* **11**: 123.
- Maranger, R., and D. F. Bird. 1995. Viral abundance in aquatic systems: A comparison between marine and fresh waters. *Mar. Ecol. Prog. Ser.* **121**: 217–226.
- Marie, D., C. P. D. Brussaard, R. Thyrhaug, G. Bratbak, and D. Vaultot. 1999. Enumeration of marine viruses in culture and natural samples by flow cytometry. *Appl. Environ. Microbiol.* **65**: 45–52.
- Mojica, K. D. A., and C. P. D. Brussaard. 2014. Factors affecting virus dynamics and microbial host-virus interactions in marine environments. *FEMS Microbiol. Ecol.* **89**: 495–515.
- Mojica, K. D. A., C. Evans, and C. P. D. Brussaard. 2014. Flow cytometric enumeration of marine viral populations at low abundances. *Aquat. Microb. Ecol.* **71**: 203–209.
- Mojica, K. D. A., J. Huisman, S. W. Wilhelm, and C. P. D. Brussaard. 2015. Latitudinal variation in virus-induced mortality of phytoplankton across the North Atlantic Ocean. *ISME J.* **10**: 500.
- Nagasaki, K., and M. Yamaguchi. 1998. Effect of temperature on the algal activity and the stability of HaV (*Heterosigma akashiwo* virus). *Aquat. Microb. Ecol.* **15**: 211–216.
- Peter, K. H., and U. Sommer. 2013. Phytoplankton cell size reduction in response to warming mediated by nutrient limitation. *PLoS One* **8**: e71528.
- Pick, F. R. 1991. The abundance and composition of freshwater picocyanobacteria in relation to light penetration. *Limnol. Oceanogr.* **36**: 1457–1462.
- Price, P. B., and T. Sowers. 2004. Temperature dependence of metabolic rates for microbial growth, maintenance, and survival. *Proc. Natl. Acad. Sci.* **101**: 4631–4636.
- Proctor, C. R., and others. 2018. Phylogenetic clustering of small low nucleic acid-content bacteria across diverse freshwater ecosystems. *ISME J.* **12**: 1344–1359.
- R Core Team. 2013. *R: A language and environment for statistical computing*. Vienna, Austria: R Foundation for Statistical Computing.
- Rolinski, S., H. Horn, T. Petzoldt, and L. Paul. 2007. Identifying cardinal dates in phytoplankton time series to enable the analysis of long-term trends. *Oecologia* **153**: 997–1008.
- Schultz, G. E., D. W. Edward III, and W. D. Hugh. 2003. Bacterioplankton dynamics in the York River estuary: Primary influence of temperature and freshwater inputs. *Aquat. Microb. Ecol.* **30**: 135–148.
- Steenhauer, L. M., and others. 2016. Isolation of cyanophage CrV infecting *Cylindrospermopsis raciborskii* and the influence of temperature and irradiance on CrV proliferation. *Aquat. Microb. Ecol.* **78**: 11–23.
- Stocker, T. 2014. *Climate change 2013: The physical science basis: Working Group I contribution to the Fifth assessment report of the Intergovernmental Panel on Climate Change*. Cambridge Univ. Press.
- Suttle, C. A. 2007. Marine viruses—Major players in the global ecosystem. *Nat. Rev. Microbiol.* **5**: 801.
- Tijdens, M., D. B. Van De Waal, H. Slovackova, H. L. Hoogveld, and H. J. Gons. 2008. Estimates of bacterial and phytoplankton mortality caused by viral lysis and microzooplankton grazing in a shallow eutrophic lake. *Freshw. Biol.* **53**: 1126–1141.
- Tomaru, Y., and K. Nagasaki. 2007. Flow cytometric detection and enumeration of DNA and RNA viruses infecting marine eukaryotic microalgae. *J. Oceanogr.* **63**: 215–221.
- van Dijk, M. A., and others. 2010. Optimizing the setup of a flow cytometric cell sorter for efficient quantitative sorting of long filamentous cyanobacteria. *Cytometry A* **77A**: 911–924.
- Velthuis, M., and others. 2017. Warming advances top-down control and reduces producer biomass in a freshwater plankton community. *Ecosphere* **8**: e01651.
- Verschoor, A. M., J. Takken, B. Massieux, and J. Vijverberg. 2003. The Limnotrons: A facility for experimental community and food web research. *Hydrobiologia* **491**: 357–377.
- Weinbauer, M. G. 2004. Ecology of prokaryotic viruses. *FEMS Microbiol. Rev.* **28**: 127–181.
- Wigington, C. H., and others. 2016. Re-examination of the relationship between marine virus and microbial cell abundances. *Nat. Microbiol.* **1**: 15024.

Wilhelm, S. W., and C. A. Suttle. 1999. Viruses and nutrient cycles in the sea: Viruses play critical roles in the structure and function of aquatic food webs. *Bioscience* **49**: 781–788.

Wommack, K. E., and R. R. Colwell. 2000. Virioplankton: Viruses in aquatic ecosystems. *Microbiol. Mol. Biol. Rev.* **64**: 69–114.

### Acknowledgments

The authors want to thank Anna Noordeloos, Suzanne Naus-Wiezer, Nico Helmsing and Erik Reichman for technical assistance. T. F. was supported by the Royal Netherlands Academy of Arts and Sciences (KNAW) and Utrecht University, and M. V. was supported by the Gieskes-Strijbis

Foundation. The work of T. F. and M. V. was furthermore supported by the International IGB Fellowship Program “Freshwater Science” of the Leibniz-Institute of Freshwater Ecology and Inland Fisheries (IGB). S. K. was supported by the Nederlandse Organisatie voor Wetenschappelijk Onderzoek (NWO) Veni grant 86312012.

*Submitted 23 September 2019*

*Revised 15 April 2020*

*Accepted 20 April 2020*